

Electronic Supplementary Information

Ligand engineering to achieve synergistic properties in 2D bilayer supertetrahedral chalcogenide cluster-based assembled material

Yan-Ling Li,^{*a} Yu-Dong Liu,^a Wei-Li Li,^a Fu-An Li,^a Yun-Xiao Feng,^a Xiao-Qiang Luo^a

and Yong-Jun Han^{*a}

^a College of Chemistry and Environmental Engineering, Pingdingshan University, Pingdingshan, 467000, China.

*E-mail: liyanling16@126.com, hanyj08@126.com

Instrumentation

Powder X-ray diffraction (PXRD) patterns of the samples were recorded using a X' Pert PRO diffractometer (Cu K α) in air at room temperature. Liquid UV-vis absorption spectra and solid-state diffuse reflectance spectra (DRS) were recorded on a UV-2550 spectrometer. BaSO₄ was applied as a 100 % reflectance references material to collect the solid-state DRS data. Steady-state photoluminescence (PL) spectra and emission decay spectroscopy were recorded on a HORIBA Scientific Fluorolog-3 spectrofluorometer equipped with an East Changing TC202 temperature controller. Luminescence spectra were measured while operating in time-correlated single photon counting (TCSPC) mode. Thermogravimetric (TG) analyses of the compounds were performed on a SDT 2960 thermal analyzer from room temperature to 800 °C at a heating rate of 10 °C/min under N₂ atmosphere. Scanning electron microscope (SEM) images and energy dispersive spectrometer (EDS) were acquired using a Zeiss Sigma 300 emission scanning electron microscope with an accelerating voltage of 0.02-30 kV for SEM images and 20 kV for EDS mapping images. The electrochemical performance and photoelectrochemical performance were measured in a three-electrode quartz cell system using a platinum plate as the counter electrode, a Ag/AgCl electrode as the reference electrode, and a sample-coated titanium foil (or glassy carbon) electrode as the working electrode, and 0.1 M Na₂SO₄ as electrolyte. The photoelectrochemical results were recorded using a CHI660E electrochemical

station. The electron spin resonance (ESR) spectra were detected using a Bruker EPR A 300-10/12 spectrometer to measure the activated species.

X-ray Crystallography

Single-crystal X-ray diffraction measurements of SCCAM-3 was performed on a Rigaku XtaLAB Pro diffractometer with Cu-K α radiation ($\lambda = 1.54184 \text{ \AA}$) at 150 K. Data collection and reduction were performed using the program CrysAlisPro.^[1] Multi-scan absorption corrections were applied to the data using CrysAlisPro.^[1] All of the structures were solved with direct methods (*SHELXS*)^[2] and refined by full-matrix least squares on F^2 using *OLEX2*,^[3] which utilizes the *SHELXL-2015* module.^[4]

All hydrogen atoms were placed in their calculated positions with idealized geometries, and they possessed fixed isotropic displacement parameters. Appropriate restraints and/or constraints were applied to the geometry, and the atomic displacement parameters of the atoms in the cluster were determined. All non-H atoms were located in the electron density and refined with anisotropic thermal parameters. SADI and DFIX were applied to keep the distances of C–S (ca. 1.85 \AA) and C–C (ca. 1.51 \AA) in reasonable range. AFIX 66 restraints were applied to keep the standard six-membered ring configuration of the phenyl group in the ligands. ISOR, RIGU and SIMU restraints were used for some atoms with large thermal motion. All structures were examined using the Addsym subroutine of PLATON to ensure that no additional symmetry could be applied to the models. A solvent mask has been used due to severely disorder of free solvent molecules around the framework and diffract weakly. According to TGA data, the solvent molecules (ca. 2 DMF) are removed through solvent mask in the refinement.

Electrode preparation

To prepare a SCCAM-3 (or T3 cluster) coated titanium foil electrode, 5 mg of SCCAM-3 (or T3 cluster) sample was mixed with 10 μL of 5 wt.% Nafion solutions and dispersed in 500 μL of ethanol. The mixture was sonicated for over 10 min to form a homogenous dispersion. The dispersion was coated onto a piece of titanium foil ($1 \times 1 \text{ cm}^2$) and dried, then a SCCAM-3 (or T3 cluster) electrode (5 mg/cm^2 of sample loading) was obtained for photoelectrochemical performance test.

A glassy carbon (GC) electrode (5 mm in diameter, $S = 0.1962 \text{ cm}^2$) was coated with SCCAM-3 (or T3 cluster) as follows: the SCCAM-3 (or T3 cluster) (5 mg) was ultrasonicated in ethanol (500

μL) and Nafion (10 μL) until a uniform ink was achieved. Then, 20 μL of the ink was pipetted onto the GC electrode surface by using a micropipettor and dried at ambient temperature, then a glassy carbon electrode coated with SCCAM-3 (or T3 cluster) was used as the working electrode for electrochemical impedance spectroscopy measurements.

Density functional theory (DFT) calculations

All-electron DFT calculations have been carried out by the latest version of ORCA quantum chemistry software^[5] (Version 5.0.3). The calculated structure was built from its single crystal structures. The PBE functional^[6] and def2-SVP basis set^[7] were adopted for optimization calculation. The DFT-D3 with BJ-damping^[8] was applied to correct the weak interaction to improve the calculation accuracy. The time-dependent DFT (TDDFT) calculation was performed with PBE0 functional^[9] and a mixed basis set (SARC-DKH-TZVP basis set^[10] for Ag/Cd atoms and the DKH-def2-SVP basis set for other atoms) at the optimized ground state geometry. The Hole-electron analysis were studied by using Multiwfn software^[11].

Experimental Section

$\text{Cd}(\text{PhS})_2$ was prepared from the reaction of molar equivalents of $\text{Cd}(\text{NO}_3)_2 \cdot 4\text{H}_2\text{O}$ and PhSNa in CH_3OH under air atmosphere.^[12] The ligand TPPA was prepared according to the literature procedures.^[13] Other reagents and solvents for synthesis were obtained from commercial sources and used without further purification.

Synthesis of $[(\text{Cd}_6\text{Ag}_4(\text{SPh})_{16}(\text{TPPA})(\text{BPE})_{0.5}) \cdot 2\text{DMF}]_n$ (SCCAM-3)

Silver nitrate (AgNO_3) (5.1 mg, 0.03 mmol) was added to a colorless solution of $\text{Cd}(\text{PhS})_2$ (20 mg, 0.06 mmol) in 3 mL DMF with stirring. After a few minutes TPPA (7 mg, 0.015 mmol) and BPE (4 mg, 0.02 mmol) was added respectively under stirring. A yellow mixture was obtained after stirring overnight and then filtered. The resulting clear yellow solution was evaporated slowly in air at room temperature. Yellow block crystals of SCCAM-3 were obtained. (Yield:81 % based on TPPA).

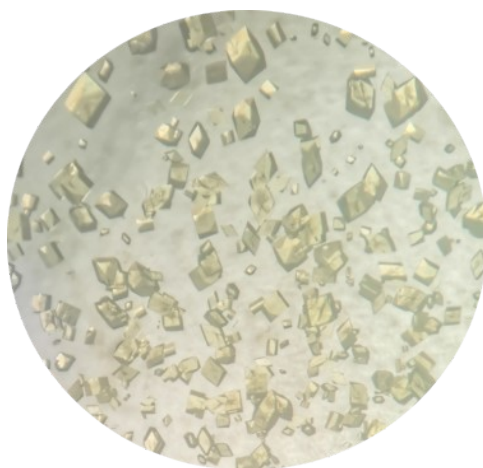


Fig. S1 Photographs of the as-synthesized SCCAM-3 crystals.

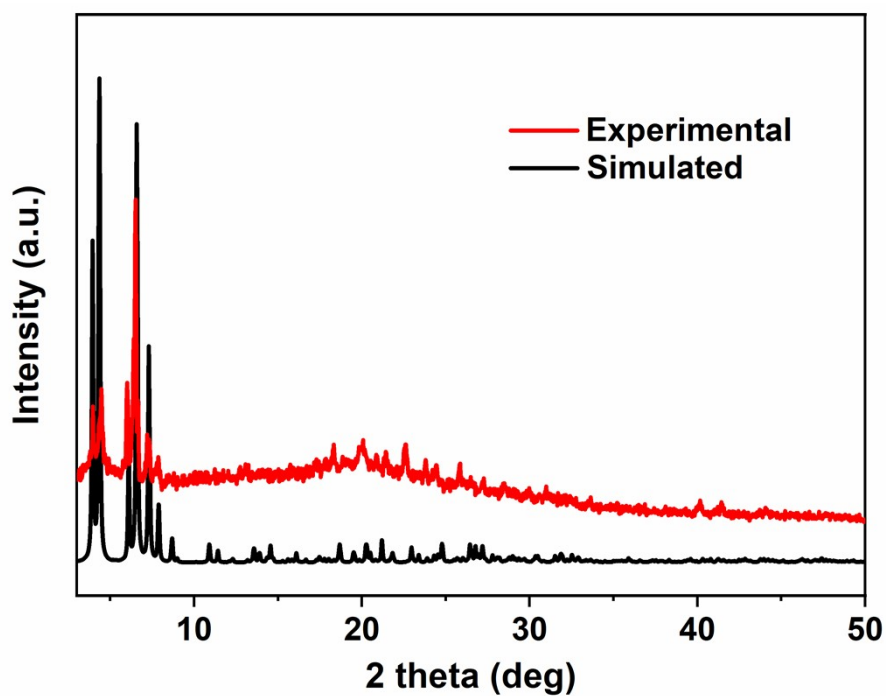


Fig. S2 Comparison of experimental and simulated powder X-ray diffraction patterns of SCCAM-3.

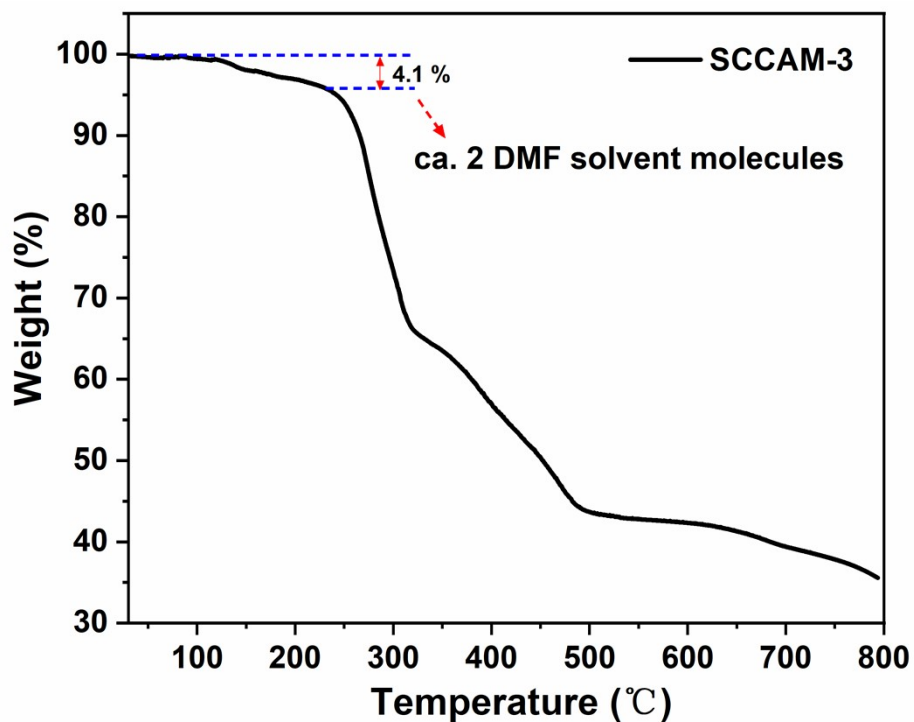


Fig. S3 The TGA curve of SCCAM-3 under N₂ atmosphere (10 °C/min). The percentage of loss mass before 232 °C is found to be 4.1%, which is assigned to the departure of two DMF molecules.

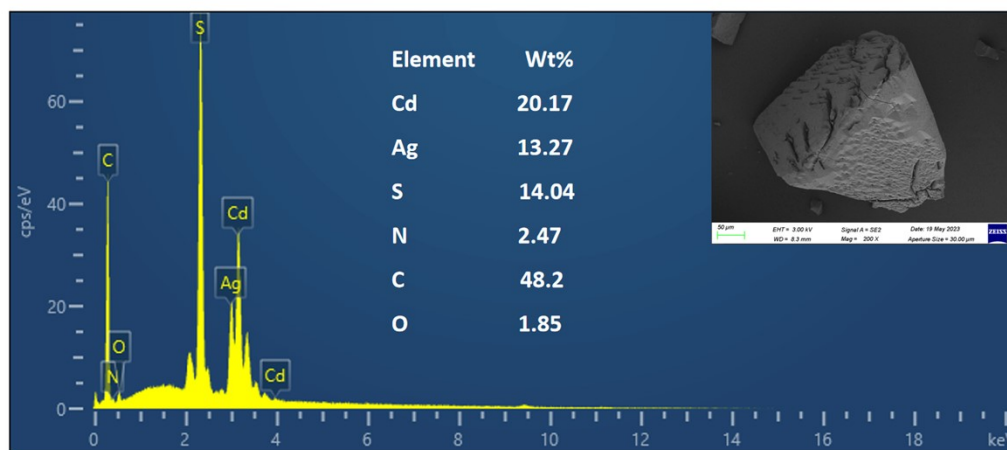


Fig. S4 The SEM image and EDS spectrum of SCCAM-3 crystals.

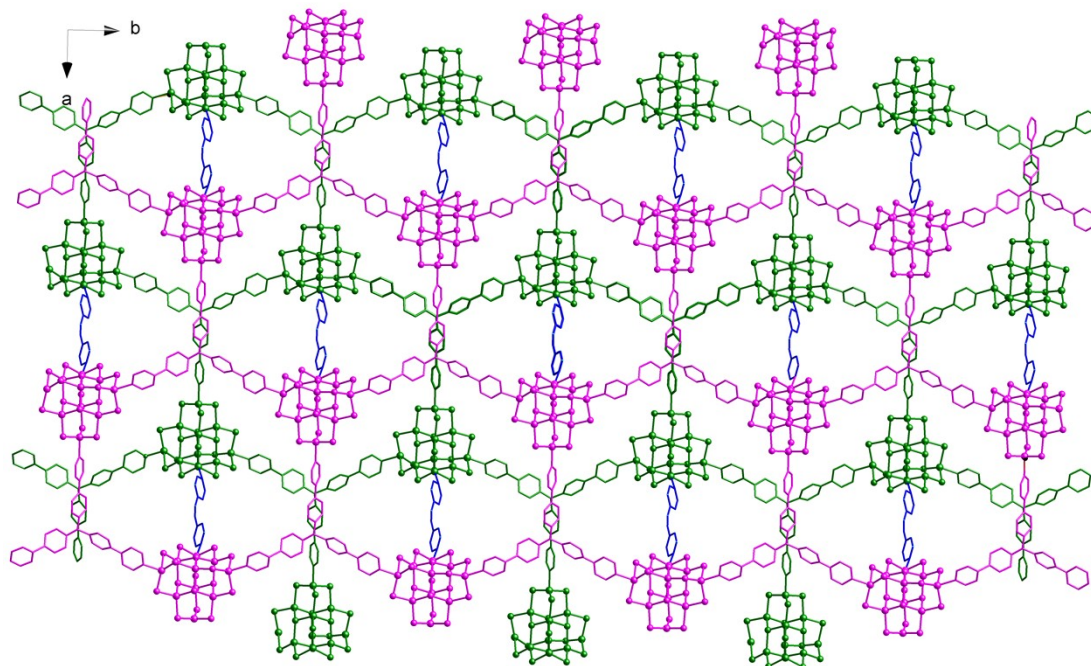


Fig. S5 The 2D bilayer (green and pink) motif in SCCAM-3 assembled by BPE (blue) of adjacent nets viewed along the c-axis.

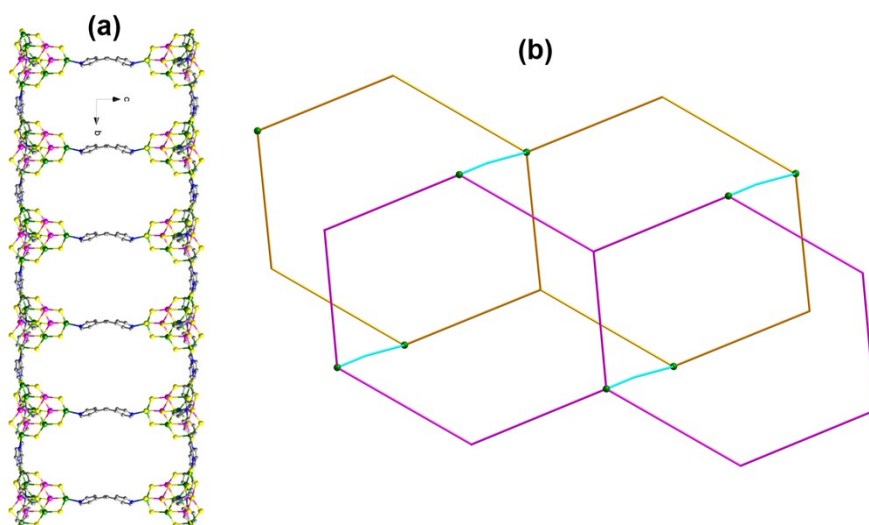


Fig. S6 (a) 2D bilayer view of SCCAM-3 along the a-direction. Phenyl groups are omitted for clarity. Color code: Cd, green; Ag, pink; S, yellow; N, blue; C, gray. (b) Schematic diagram of the extended 2D bilayer topology (green: T3 clusters; triangular linker: TPPA ligands; turquoise linker: BPE ligands).

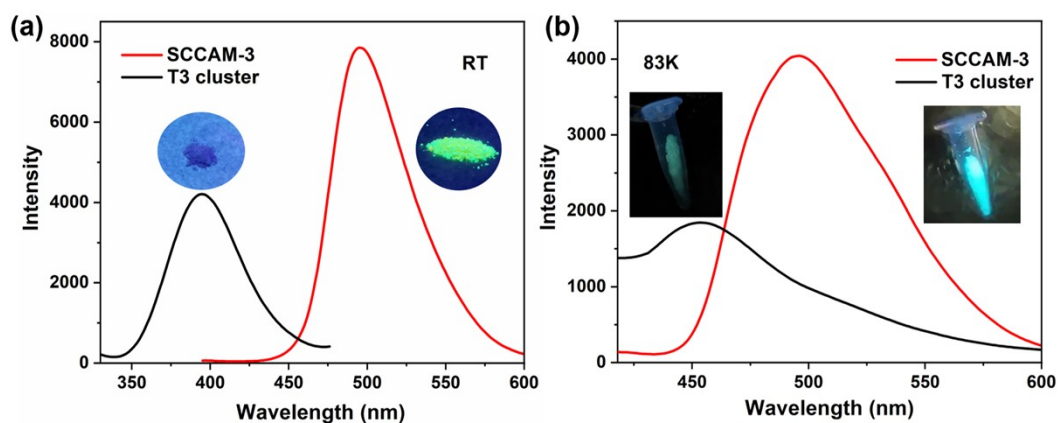


Fig. S7 The emission intensity of the SCCAM-3 and T3 cluster at room temperature (a) and 83 K (b). The inset shows the luminescence colors images of SCCAM-3 and T3 cluster under UV (365 nm) lamp.

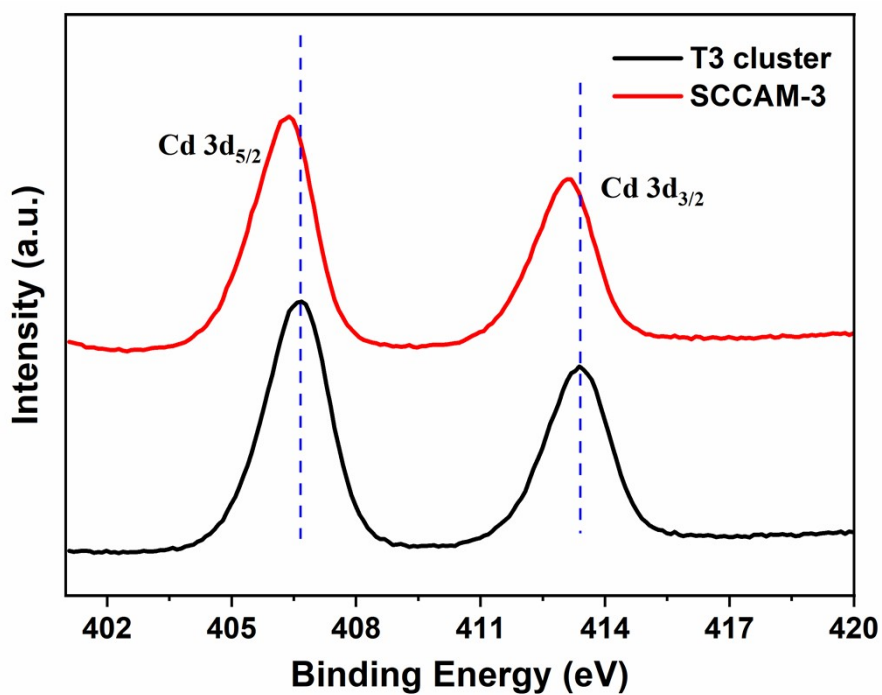


Fig. S8 The XPS spectra of the Cd element for SCCAM-3 and T3 cluster.

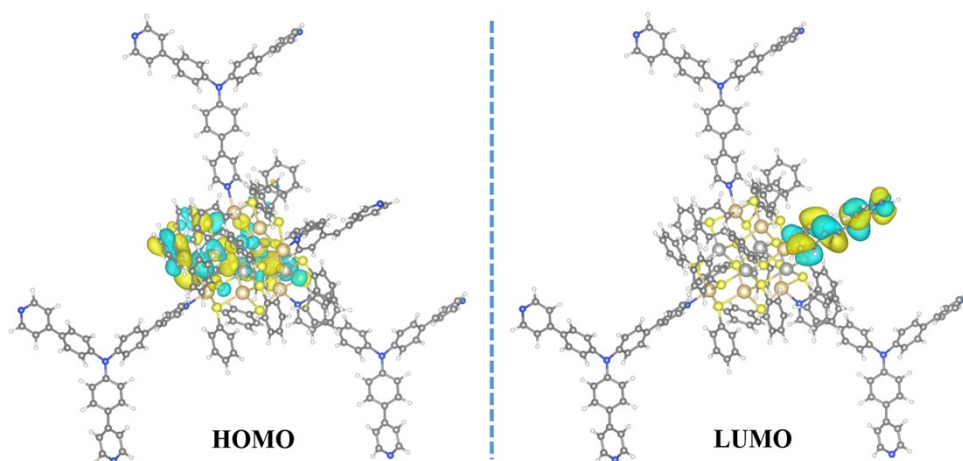


Fig. S9 DFT calculation of HOMO and LUMO for SCCAM-3.

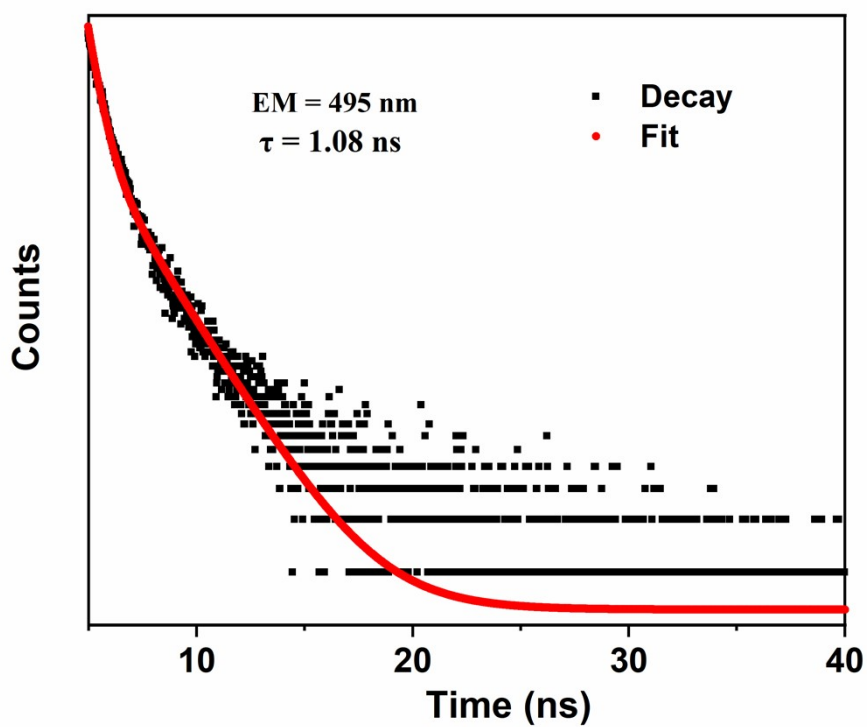


Fig. S10 Photoluminescence decay profile of SCCAM-3 measured at 495 nm at RT using 375 Laser.

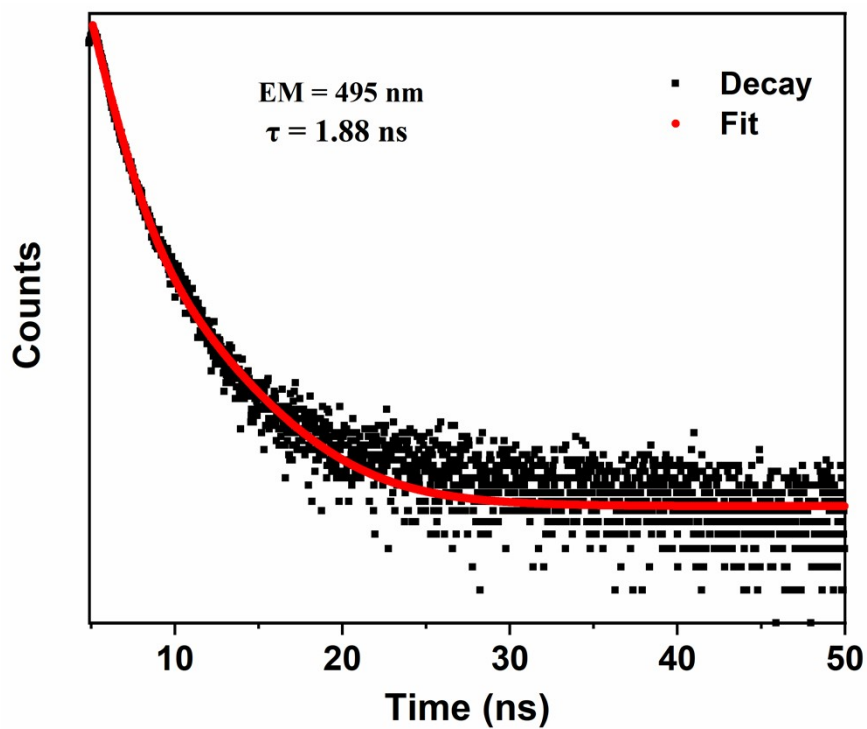


Fig. S11 Photoluminescence decay profile of SCCAM-3 measured at 495 nm at 83 K using 375 Laser.

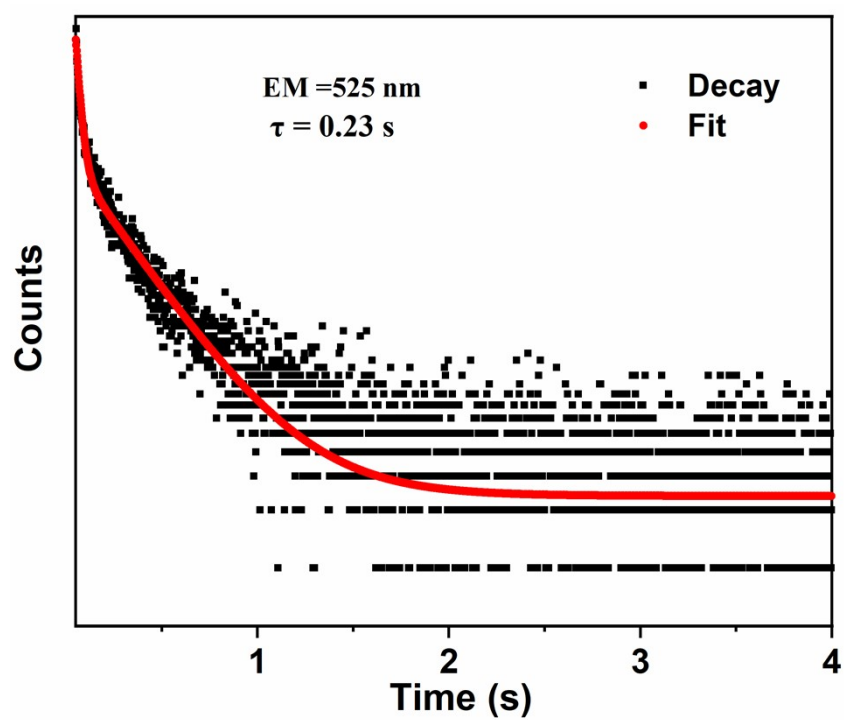


Fig. S12 Photoluminescence decay profile of SCCAM-3 measured at 525 nm at 83 K using 355 nm SpectralLed.

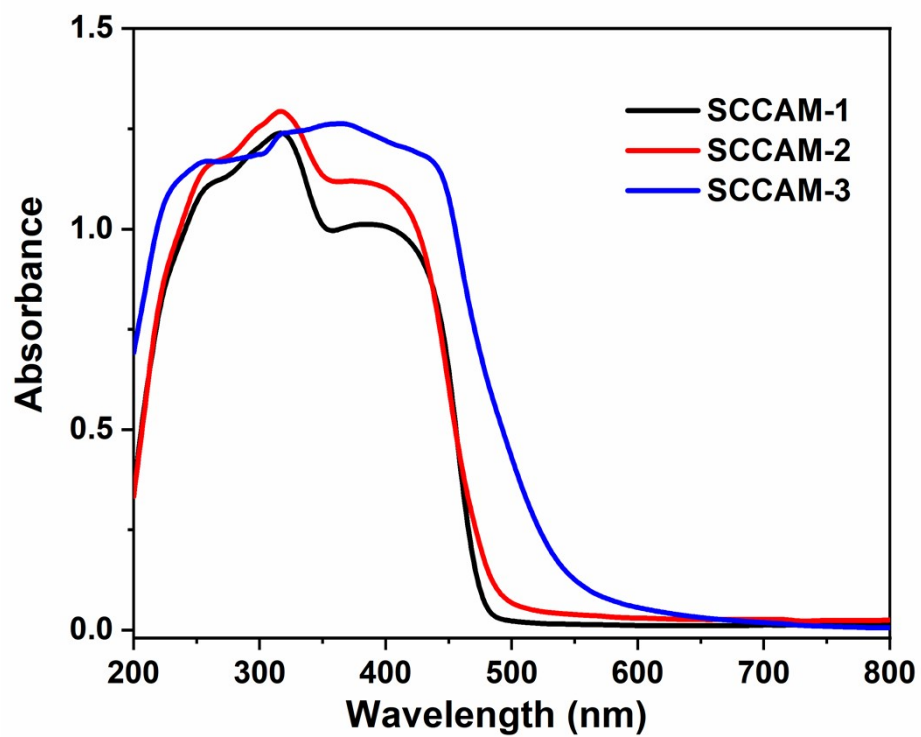


Fig. S13 Solid-state Uv/vis diffuse spectra of the SCCAM-1, -2 and -3. The spectra of SCCAM-1 and -2 were reproduced with permission from ref 8. Copyright 2023 American Chemical Society.

Table S1 Crystal data for SCCAM-3.

Compound	SCCAM-3
CCDC number	2172629
Empirical formula	C ₁₄₁ H ₁₂₃ Ag ₄ Cd ₆ N ₇ S ₁₆ O ₂
Formula weight	3566.30
Temperature/K	150
Crystal system	monoclinic
Space group	I2/m
a /Å	15.64080(10)
b /Å	26.8262(2)
c /Å	40.7797(4)
α /°	90
β /°	90.1560(10)
γ /°	90
Volume/Å ³	17110.4(2)
Z	4
ρ _{calc} g/cm ³	1.384
μ/mm ⁻¹	11.593
F(000)	7064.0
Radiation	CuKα (λ = 1.54184)
2θ range for data collection/°	6.046 to 146.344
Index ranges	-19 ≤ h ≤ 19, -25 ≤ k ≤ 33, -50 ≤ l ≤ 50
Reflections collected	93941
Independent reflections	17298 [R _{int} = 0.0445, R _{sigma} = 0.0354]
Data/restraints/parameters	17298/2134/1074
Goodness-of-fit on F ²	1.027
Final R indexes [I >= 2σ (I)]	R ₁ = 0.0948, wR ₂ = 0.2929
Final R indexes [all data]	R ₁ = 0.1031, wR ₂ = 0.3031
Largest diff. peak/hole / e Å ⁻³	1.78/-1.53

$$R_1 = \sum ||F_o| - |F_c|| / \sum |F_o|. \quad wR_2 = [\sum w(F_o^2 - F_c^2)^2 / \sum w(F_o^2)^2]^{1/2}$$

Photocatalysis measurement

Crystalline SCCAM-3 and T3 clusters were applied as photocatalysts for degradation of tetracycline (TC) in aqueous solution under visible light illumination. A 300 W Xenon lamp equipped with a cut-off filter ($\lambda > 400$ nm) was used as a light source. Typically, 25 mg of the photocatalyst was dispersed in 30 mL of TC aqueous solution (4.5×10^{-5} M, 20 mg L^{-1}). The mixture was stirred for 1 h in the dark to afford a homogeneous suspension before the analysis. The distance between the liquid level and the lamp was adjusted to ~ 5 cm. The suspension was then irradiated by light during stirring. Aliquots of 1 mL were withdrawn from the suspension at an interval of 5 min. The dispersed catalyst in the withdrawn mixture was removed by centrifugation and the concentration of TC in the clear sample solution was monitored by measuring the absorption intensity at the maximum absorption wavelength of $\lambda=357$ nm by UV-vis spectrophotometer.

For the cyclic photocatalysis test, the catalyst was collected after each cycle. The recycled solid was washed by water several times and then reused as catalyst for photocatalytic degradation of the TC solution. For the photocatalytic mechanism studies, radical scavengers of isopropanol ($60 \mu\text{L/mL}$), ammonium oxalate (0.142 mg/mL), and nitrotetrazolium blue chloride (0.096 mg/mL) was added to the parallel reactions separately.

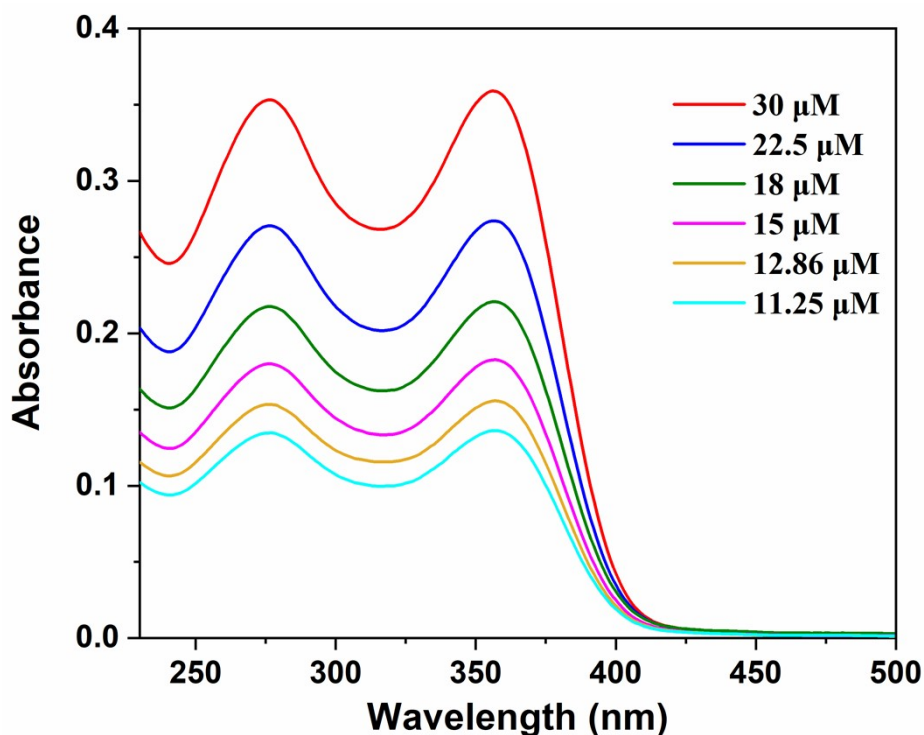


Fig. S14 UV-vis absorption spectra of TC upon different solution concentration.

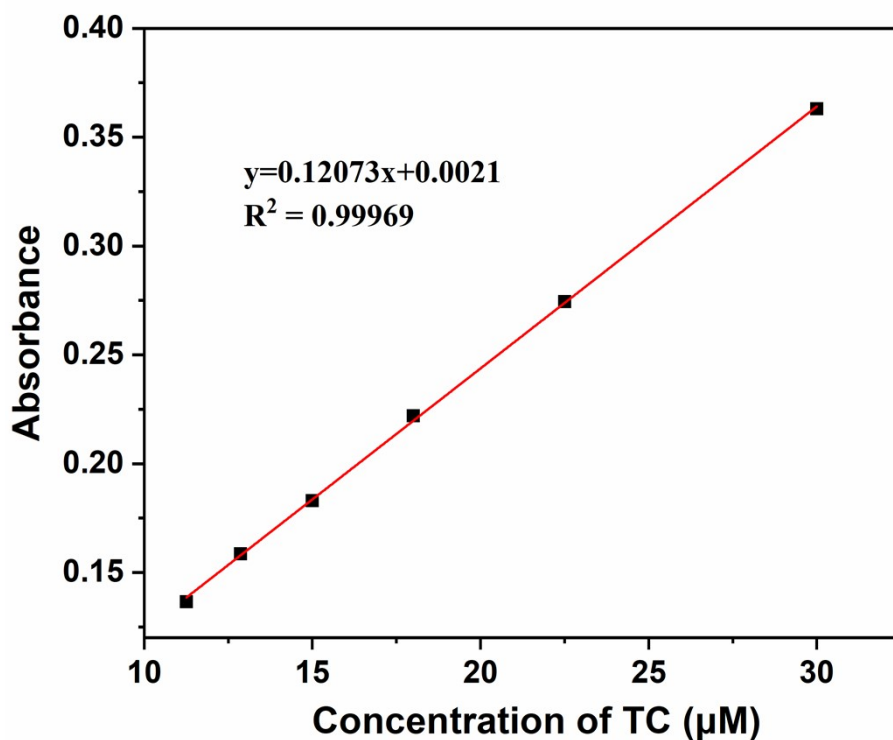


Fig. S15 UV-vis absorption intensity of TC solution at 357 nm upon different solution concentration, the solid line is linearly fitted.

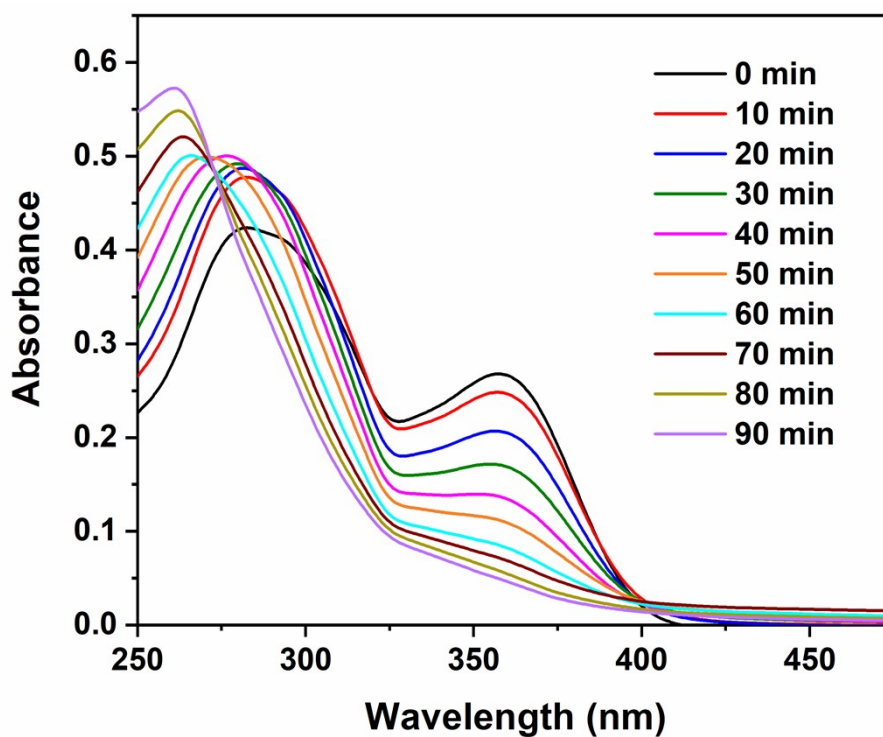


Fig. S16 UV-vis spectra of the aqueous TC (4.5×10^{-5} M) during the degradation process photocatalyzed by SCCAM-3.

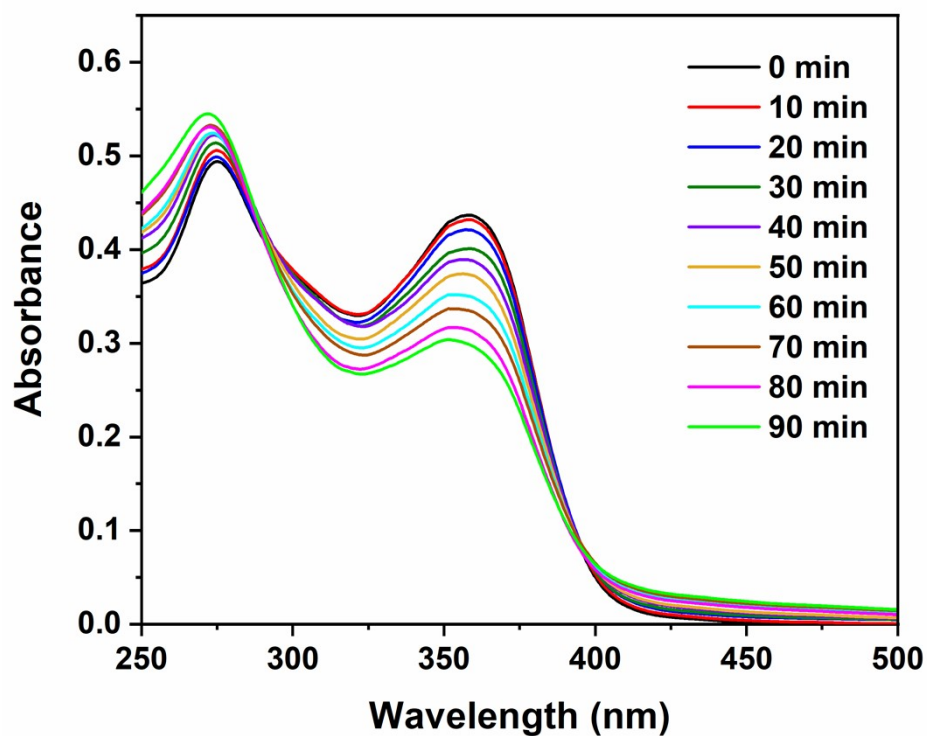


Fig. S17 UV/vis spectra of the aqueous TC (4.5×10^{-5} M) during the degradation process photocatalyzed by T3 cluster.

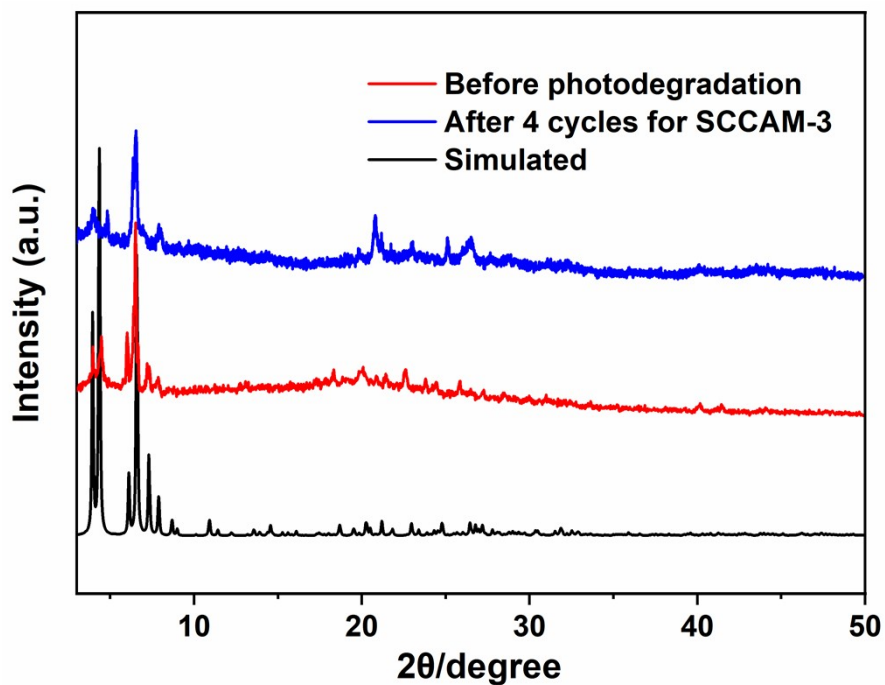


Fig. S18 The PXRD patterns of SCCAM-3 before and after TC degradation for four cycles.

Reference

- [1] CrysAlisPro 2012, Agilent Technologies. Version 1.171.36.31.
- [2] G. M. Sheldrick, *Acta Cryst. A*, 2008, **64**, 112-122.
- [3] O. V. Dolomanov, L. J. Bourhis, R. J. Gildea, J. A. K. Howard and H. Puschmann, *J. Appl. Cryst.*, 2009, **42**, 339-341.
- [4] G. M. Sheldrick, *Acta Cryst. A*, 2015, **71**, 3-8.
- [5] F. Neese, Software update: The ORCA program system, version 4.0. *Wiley Interdiscip. Rev. Comput. Mol. Sci.* 2017, **8**, e1327.
- [6] J. P. Perdew, K. Burke, M. Ernzerhof, Generalized gradient approximation made simple. *Phys. Rev. Lett.*, 1996, **77**, 3865-3868.
- [7] F. Weigend, R. Ahlrichs, Balanced basis sets of split valence, triple zeta valence and quadruple zeta valence quality for H to Rn: Design and assessment of accuracy. *Phys. Chem. Chem. Phys.*, 2005, **7**, 3297-3305.
- [8] S. Grimme, S. Ehrlich, L. Goerigk, Effect of the damping function in dispersion corrected density functional theory. *J. Comp. Chem.* 2011, **32**, 1456-1465.
- [9] C. Adamo, V. Barone, Toward reliable density functional methods without adjustable parameters: The PBE0 model. *J. Chem. Phys.*, 1999, **110**, 6158-6170.
- [10] J. D. Rolfes, F. Neese, D. A. Pantazis, All-electron scalar relativistic basis sets for the elements Rb-Xe. *J. Comput. Chem.*, 2020, **41**, 1842-1849.
- [11] T. Lu, F. Chen, Multiwfn: A multifunctional wavefunction analyzer. *J. Comput. Chem.*, 2012, **33**, 580-592.
- [12] I. G. Dance, R. G. Garbutt, D. C. Carig, M. L. Scudder, *Inorg. Chem.* 1987, **26**, 4057-4064.
- [13] M. D. Zhang, C. M. Di, L. Qin, X. Q. Yao, Y.-Z. Li, Z.-J. Guo, H.-G. Zheng, *Cryst. Growth Des.*, 2012, **12**, 3957-3963.